NeuroImage 49 (2010) 1820–1830

Contents lists available at ScienceDirect

NeuroImage

journal homepage: www.elsevier.com/locate/ynimg

CSF biomarker pathology correlates with a medial temporo-parietal network affected by very mild to moderate Alzheimer's disease but not a fronto-striatal network affected by healthy aging

Anders M. Fjell [a,b,*], Inge K. Amlien [a], Lars T. Westlye [a], Vidar Stenset [c,d], Tormod Fladby [c,d], Anders Skinningsrud [e], Dag E. Eilsertsen [f], Atle Bjørnerud [a,g,h], Kristine B. Walhovd [a,b]

[a] Center for the Study of Human Cognition, Department of Psychology, University of Oslo, Norway
[b] Department of Neuropsychology, Ullevaal University Hospital, Norway
[c] Department of Neurology, Akershus University Hospital, Norway
[d] Department of Neurology, Faculty Division Akershus University Hospital, University of Oslo, Norway
[e] Department of Clinical Chemistry and Nuclear medicine, Akershus University Hospital, Norway
[f] Department of Psychology, University of Oslo, Norway
[g] Rikshospitalet University Hospital, Department of Radiology, Norway
[h] Department of Physics, University of Oslo, Norway

ARTICLE INFO

Article history:
Received 4 May 2009
Revised 20 August 2009
Accepted 16 September 2009
Available online 30 September 2009

Keywords:
Aβ42
Cerebral cortex
Hippocampus
Magnetic resonance imaging
Tau proteins

ABSTRACT

It is suggested that reductions in a medial temporo-parietal episodic memory network characterize Alzheimer's disease (AD), while changes in a fronto-striatal executive network characterize healthy aging. In the present study, magnetic resonance imaging (MRI) was used to test this directly. MRI scans of 372 participants from two samples were analyzed: Sample 1 consisted of 96 very mild to moderate AD patients, 93 healthy elderly (HE), and 137 young (HY), all with available MR scans, while Sample 2 consisted of 46 MCI patients, with available MR scans and measures of CSF biomarkers Aβ42 and tau protein. Substantial morphometric reductions of the medial temporo-parietal network were found in AD, while the fronto-striatal network was less affected. Both networks were affected by healthy aging, but the fronto-striatal to a greater degree than the medial temporo-parietal. Further exploratory analyses of 49 cortical and subcortical structures indicated no overlap between predictors of AD vs. HE and predictors of HE vs. HY. CSF biomarker pathology correlated with the medial temporo-parietal but not fronto-striatal network. Likewise, the AD-prone structures from the exploratory analyses were related to CSF biomarkers, while the aging-prone structures were not. It is concluded that the pattern of macrostructural brain changes in very mild to moderate AD can be clearly delineated from that of healthy aging.

© 2009 Elsevier Inc. All rights reserved.

Introduction

Alzheimer's disease (AD) is associated with a range of structural brain changes that can be measured in vivo. These effects are especially prominent in a medial temporo-parietal neural network involved in episodic memory function (Buckner and Wheeler, 2001), which includes the hippocampus (de Leon et al., 1989; Fischl et al., 2002; Jack et al., 1992; Thompson et al., 2007), entorhinal, retrosplenial, posterior cingulate and precuneus cortices, while frontal effects are more moderate in early stages of the disease (Dickerson et al., 2008, 2009; Du et al., 2007; Fennema-Notestine et al., 2009; Fjell et al., 2008b; Lerch et al., 2008, 2005; McEvoy et al., 2009; Singh et al., 2006; Thompson et al., 2003). Until recently, the medial parietal parts of this network (retrosplenial, posterior cingulate, precneus) have received less attention than hippocampus and entorhinal cortex in the structural brain imaging literature. This is opposed to PET studies, where reduced medial parietal metabolism (Mosconi et al., 2007) and Aβ pathology (Frisoni et al., 2009), especially in posterior cingulate and precuneus, are established.

Structural MRI has been suggested as a criterion for AD diagnosis (Dubois et al., 2007). However, there is still considerable uncertainty regarding whether and to what extent brain changes observed in AD overlap with changes associated with healthy aging (Arriagada et al., 1992; Brayne and Calloway, 1988; Whalley, 2002), and to what extent they are specific to AD (Buckner, 2004; Head et al., 2005; Ohnishi et al., 2001). AD is an age-related disease, and the brain changes in AD are seen on top of the brain changes observed in healthy aging. This makes it difficult to distinguish atrophy related to AD from atrophy that is common among elderly, whether they have AD or not. For instance, morphometric brain changes, e.g. of hippocampus, are also seen in healthy elderly of advanced age (Walhovd et al., in press-b). Thus, although the atrophy rates are much higher in AD than in

* Corresponding author. Department of Psychology, Pb. 1094 Blindern, 0317 Oslo, Norway. Fax: +47 22 84 50 01.
E-mail address: andersmf@psykologi.uio.no (A.M. Fjell).

1053-8119/$ – see front matter © 2009 Elsevier Inc. All rights reserved.
doi:10.1016/j.neuroimage.2009.09.029

healthy aging, the evidence for specific macrostructural brain changes distinguishing AD from healthy aging is limited, even though the entorhinal and the medial parietal cortices generally are found to be among the best preserved cortical regions in healthy aging (Fjell et al., 2009). While degeneration of the medial temporo-parietal memory network has been suggested to be more vulnerable in AD than other networks or areas, the fronto-striatal network supporting executive functions has been proposed as the network that is most affected by healthy aging (Buckner, 2004; Head et al., 2005). A range of morphometric studies have pointed to the selective vulnerability of anterior cortical brain areas in healthy aging (Allen et al., 2005; Fjell et al., 2009; Raz et al., 1997, 2007; Salat et al., 2004). Still, this is a complicated issue, since also prefrontal atrophy is seen in MCI/AD relative to healthy elderly, at least in advanced stages of the disease (Du et al., 2007; Fennema-Notestine et al., 2009). However, while the striatal part of the circuit has been found to be affected by non-pathological aging processes (Walhovd et al., in press-b), it is generally not more atrophic (Cousins et al., 2003) in AD compared to healthy aging.

As argued above, the possibility of identifying clear and clinically useful differences is unavoidably challenged by the intrinsic relationship between aging and AD. Given the substantial morphometric brain changes even in healthy aging, it may not be realistic to identify single structures that show selective vulnerability to AD only. However, specific brain changes in AD may be identified by the patterns of change across different neural circuits (Head et al., 2005). To clarify the question of how unique the effects of AD are, direct comparisons of effects of AD with effects of healthy aging, across several areas and circuits simultaneously, are necessary. In one such study, age-related decline was observed in volume of the prefrontal cortices, insula, anterior cingulate, superior temporal gyrus, inferior parietal lobes, and precuneus, while AD patients had reductions of volume in the hippocampal formation and entorhinal cortices (Ohnishi et al., 2001).

It has been argued that temporal and hippocampal atrophy in MCI/AD is secondary to pathological depositions of extracellular Aβ42 (Arriagada et al., 1992; Thal et al., 2002) and intracellular neurofibrillary tangles (NFT) (Price and Morris, 1999). NFTs are composed of tau proteins and originate in the entorhinal cortex and adjacent limbic structures (Braak and Braak, 1996; Mesulam, 1999), including hippocampus, thus affecting vital parts of the medial temporo-parietal circuit even early in the disease (Petersen et al., 2006). Aβ42 deposition is probably more distributed (Edison et al., 2007; Guillozet et al., 2003; Rowe et al., 2007), but will eventually also affect areas in the medial temporo-parietal circuit (Braak and Braak, 1991). CSF biomarker pathology is a relevant diagnostic criterion for AD (Dubois et al., 2007), and was included in the study to validate MRI findings.

The present paper reports the results of two independent studies, and has three aims. In Study 1, we wanted to test whether a dissociation of morphometric changes in the medial temporo-parietal vs. the fronto-striatal network can be found in very mild to moderate AD vs. healthy aging. Hippocampal volume, and thickness of the entorhinal, retrosplenial, posterior cingulate and precuneus cortices were included in the medial temporo-parietal network, while the superior frontal cortices, putamen, and caudate were regarded as structures of the fronto-striatal network (Fig. 1). No previous studies have directly tested the selective vulnerability of these predefined neural networks, and compared the classification accuracy of each. Further, we wanted to explore whether additional cortical and subcortical structures could differentiate effects of AD from effects of healthy aging. To reach this aim, volume of 16 subcortical and thickness of 33 cortical regions were measured. The aim of Study 2 was to validate the MRI results against tau and Aβ42. Our hypothesis was that correlations between CSF biomarker pathology (Aβ42, tau) and morphometry would be present for the medial temporo-parietal but not the fronto-striatal circuit. From the exploratory analysis, we expected the cluster of structures that best distinguished very mild to moderate AD from HE to correlate with CSF biomarker pathology, but not the cluster that best distinguished HE and HY. By this approach we hoped (1) to validate the morphometric effects using other biomarkers related to AD and (2) to test whether the conclusions could be generalized by using the results from one sample to guide the analyses in an independent sample.

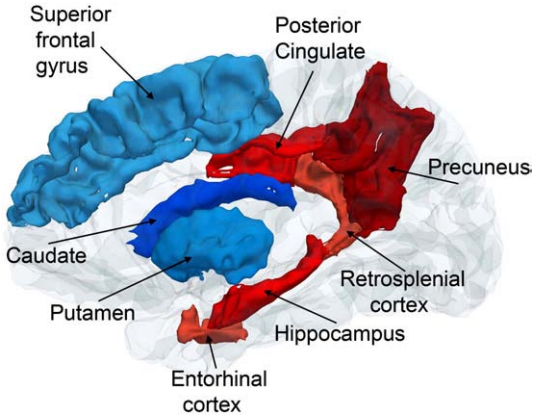

Fig. 1. The medial temporo-parietal and the fronto-striatal circuits. The figure shows the 3D renderings of the segmentation results for one arbitrary chosen participant for the structures included in the medial temporo-parietal (red) and the fronto-striatal (blue) networks targeted in the present study.

Materials and methods

Sample

This project was based on two independent studies, and sample characteristics for the participants included are presented in Table 1. Participants' consent was obtained according to the Declaration of Helsinki and the ethical committee of the institution in which the work was performed has approved it.

Study 1: The raw data were acquired from the Open Access Series of Imaging Studies (www.oasis-brains.org), a database that has been used in previous studies (Buckner et al., 2004, 2005; Dickerson et al., 2008; Fotenos et al., 2005; Marcus et al., 2007). All MR-data were processed exclusively for the present study (see below), and the analyses included in the present paper have to our knowledge not previously been reported. Details of recruitment and screening procedures are given by Marcus et al. (2007). The HY participants (<60 years) were interviewed about medical history and use of psychoactive drugs, while elderly participants (>60 years) underwent the Washington University Alzheimer Disease Research Center's full clinical assessment, yielding clinical dementia rating (CDR) for all participants (Berg, 1984, 1988; Morris, 1993; Morris et al., 2001). A global CDR of 0 was taken to indicate no dementia (HE group), and CDRs of 0.5 or higher to indicate very mild to moderate AD. Participants were excluded if they suffered from other active neurological or psychiatric illness, serious head injury, history of clinically meaningful stroke, use of psychoactive drugs, or had gross anatomical abnormalities evident from MRI images. During processing in the laboratory of the present authors, four of the AD patients were excluded due to less than optimal scan quality, yielding 97 AD patients. Ninety-three healthy and age-matched HE with high quality MR scans were selected, in addition to 137 young participants (18–29 years).

Study 2: Patients aged 40–79 years with MCI (Gauthier et al., 2006) established for at least 6 months attending a university-based clinic in Norway between September 2005 and December 2007 were assessed for inclusion. Criteria for inclusion were symptoms lasting ≥6 months, Global Detoriation Scale score (GDS) (Auer and Reisberg,

Table 1
Sample characteristics.

	Study 1			Study 2
	Mild AD	Healthy Elderly	Young	MCI
Participants	96	93	137	46
Sex (f/m)	59/37	69/24	77/60	21/25
Age	76.6 (62–96)	76.7 (61–94)	22.2 (18–29)	61.4 (43–78)
Education[a]	2.8 (1–5)	3.3 (1–5)*	NA	12.5 yrs (7–19)
SES	2.8 (1–5)[b]	2.5 (1–5)[c]	NA	NA
MMSE	24.4 (14–30)	28.9 (25–30)**	NA	27.8[d] (23–30)
CDR	0.66 (0.5–2.0)	0**	NA	0.5 0.5–0.5
T-tau pato[e]	NA	NA	NA	13
Aβ42 pato[e]	NA	NA	NA	9

NA: information not available.
*$p < .05$ for mild AD vs. healthy elderly.
**$p < 10^{-18}$.
[c]Available for 92 participants only.
[a] Available for all participants > 60 years, and sporadically for the rest. 1: less than high school graduate, 2: high school graduate, 3: some college, 4: college graduate, 5: beyond college.
[b] Available for 79 participants only.
[d] Available for 43 participants only.
[e] Number with pathological levels.

1997; Reisberg et al., 1988) from 2 to 3 as determined from a clinical interview and screening tests (Mini Mental Status Examination [MMSE] (Folstein et al., 1975), STEP parameters 13–20 and fluency, interference, numeral–letter items from the I-flex (Royall et al., 1992; Wallin et al., 1996) and Cognistat (Kiernan et al., 1987)). All patients had CDR = 0.5. Criteria for exclusion were impaired activities of daily living (SDL), established psychiatric disorder, cancer, drug abuse, solvent exposure or anoxic brain damage. Forty-six patients satisfied all criteria, and successfully underwent MR and lumbar puncture.

MRI acquisition

Study 1: For each subject, 3–4 individual T1-weighted magnetization prepared rapid gradient-echo (MP-RAGE) images, optimized for gray–white contrast, were acquired on a 1.5-T Vision scanner (Siemens, Erlangen, Germany): TR = 9.7 ms, TE = 4.0 ms, flip angle = 10°, TI = 20 ms, TD = 200 ms, sagittal orientation, thickness = 1.25 mm, gap = 0 mm, 128 slices, with 256 × 256 pixels (1 × 1 mm) resolution. Head movement was minimized by cushioning and a thermoplastic face mask (Marcus et al., 2007).

Study 2: MR scans were from two sites (site 1: 17, site 2: 29): site 1: Siemens Symphony 1.5 T with a conventional quadrature head coil. Two MP-RAGE, T1-weighted sequences in succession (TR/TE/TI/FA = 2730 ms/3.19 ms/1100 ms/15°, matrix = 256 × 192), 128 sagittal slices, thickness = 1.33 mm, in-plane resolution of 1.0 mm × 1.33 mm; site 2: Siemens Espree 1.5 T; 3D MP-RAGE, T1-weighted sequence, TR/TE/TI/FA = 2400/3.65/1000/8°, matrix = 240 × 192, 160 sagittal slices, thickness = 1.2 mm, in-plane resolution of 1 mm × 1.2 mm. As described in another publication, six controls were scanned on both scanners, showing that change of scanner was unlikely to introduce bias in the data (Fjell et al., 2008b). A newly developed atlas normalization procedure was used, increasing the robustness and accuracy of the segmentations across different scanners (Han and Fischl, 2007).

MRI analysis

MRI data were analyzed at the Neuroimaging Analysis Lab at the Center for the Study of Human Cognition, University of Oslo, by use of FreeSurfer 4.01 (http://surfer.nmr.mgh.harvard.edu/). For subcortical structures, a neuroanatomical label was automatically assigned to each voxel based on probabilistic information automatically estimated from a manually labeled training set (Fischl et al., 2002). The technique has been shown to be comparable in accuracy to manual labeling (Fischl et al., 2002, 2004a). As part of this procedure, a measure of cortical GM volume was estimated, which was included in the subcortical volume analyses. Intracranial volume (ICV) was estimated by use of an atlas-based normalization procedure (Buckner et al., 2004). Cortical thickness measurements were obtained by reconstructing representations of the gray–white matter boundary and the cortical surface (Dale et al., 1999; Dale and Sereno, 1993), and the distance between these surfaces at each point across the cortical mantle was calculated. The maps produced are capable of detecting submillimeter differences between groups (Fischl and Dale, 2000), which has been validated using histology and MR (Kuperberg et al., 2003; Rosas et al., 2002). Maps were smoothed using a circularly symmetric Gaussian kernel across the surface with an FWHM of 15 mm and averaged across participants using a non-rigid high-dimensional spherical averaging method to align cortical folding patterns (Fischl et al., 1999). This procedure provides accurate matching of morphologically homologous cortical locations among participants on the basis of each individual's anatomy while minimizing metric distortion, resulting in a measure of cortical thickness for each person at each point on the reconstructed surface. An automated labeling system was used to divide the cortex into 33 different gyral-based areas in each hemisphere (Desikan et al., 2006; Fischl et al., 2004b), and mean thickness within each was used in the analyses. Note that the label "retrosplenial cortex" used in the present paper refers to the label "isthmus cingulate" in the atlas.

The thickness estimation procedure is automated, but we routinely check the accuracy of the spatial registration and the WM and GM segmentations manually. The types of errors that most often require user intervention are insufficient removal of non-brain tissue (typically dura in superior brain areas) and inclusion of vessels adjacent to the cortex (especially in the temporal lobes). These types of errors are limited in spatial extension, typically seen in a minor area of the brain in a few slices, but are nevertheless routinely corrected by manual interventions.

Selection of ROIs

Hippocampal volume, and thickness of the entorhinal, retrosplenial, posterior cingulate and precuneus cortices were included in the medial temporo-parietal network, while the superior frontal cortices, putamen, and caudate were regarded as structures of the fronto-striatal network. Parahippocampal cortices are also implied in episodic memory processing, but have been found to be less affected in MCI/early AD than the entorhinal cortex (Dickerson et al., 2008; Du et al., 2007). Lateral parietal areas are affected by AD (Dickerson et al., 2008; Du et al., 2007), and probably also play a part in memory

Table 2
Univariate analysis of variance.

Structure	Volume controls, mean (SD)	Volume AD mean (SD)	Volume young mean (SD)	AD vs. Controls		Young vs. Controls	
				F	*p* <	*F*	*p* <
Third ventricle	0.37 (0.96)	0.73 (0.92)	−0.76 (0.34)	**8.13**	**.005**	**158.26**	**10^{-27}**
Fourth ventricle	0.22 (1.05)	−0.09 (0.99)	−0.08 (0.95)	**4.23**	**.05**	**5.05**	**.05**
Brainstem	−0.22 (0.98)	−0.26 (0.98)	0.33 (0.93)	0.09	n.s.	**18.76**	**10^{-4}**
CSF	0.13 (0.53)	0.51 (1.55)	−0.45 (0.35)	**5.29**	**.05**	**98.44**	**10^{-18}**
Lateral ventricle	0.42 (0.75)	0.79 (0.94)	−0.84 (0.32)	**9.66**	**.005**	**306.91**	**10^{-43}**
Inferior lateral ventricle	0.10 (0.76)	0.94 (1.07)	−0.73 (0.18)	**47.61**	**10^{-10}**	**151.23**	**10^{-26}**
Cerebellum WM	−0.38 (0.91)	−0.47 (0.95)	0.58 (0.77)	0.48	n.s.	**74.38**	**10^{-14}**
Cerebellum cortex	−0.44 (0.74)	−0.60 (0.83)	0.72 (0.79)	2.53	n.s.	**125.74**	**10^{-22}**
Thalamus	−0.45 (0.56)	−0.80 (0.88)	0.87 (0.54)	**11.01**	**.005**	**323.77**	**10^{-44}**
Caudate	−0.19 (1.02)	−0.14 (1.17)	0.23 (0.79)	0.12	n.s.	**12.42**	**.001**
Putamen	−0.57 (0.71)	−0.77 (0.59)	0.92 (0.54)	**4.85**	**.05**	**325.14**	**10^{-45}**
Pallidum	−0.55 (0.73)	−0.66 (0.74)	0.84 (0.65)	1.24	n.s.	**229.15**	**10^{-35}**
Hippocampus	−0.18 (0.70)	−1.00 (0.77)	0.82 (0.48)	**75.97**	**10^{-14}**	**163.24**	**10^{-27}**
Amygdala	−0.21 (0.72)	−0.92 (0.76)	0.78 (0.61)	**45.35**	**10^{-9}**	**125.34**	**10^{-22}**
Accumbens	−0.48 (0.56)	−0.83 (0.63)	0.91 (0.65)	**17.51**	**10^{-4}**	**284.29**	**10^{-41}**
Cerebral WM	−0.27 (0.91)	−0.76 (0.83)	0.72 (0.60)	**20.34**	**10^{-4}**	**98.00**	**10^{-18}**
Cerebral cortex	−0.53 (0.53)	−0.91 (0.51)	1.00 (0.48)	**27.00**	**10^{-6}**	**523.53**	**10^{-60}**

The volumes included are corrected for ICV, and the statistics are done on the residuals (*z*-scores). Comparisons are done between AD patients and age-matched controls, and between controls and young participants. Age was included as covariate in the analyses of AD vs. HE. Ventricular variables were larger in AD than HE, and larger in HE than young. For all other measures the opposite pattern was observed.
Bold characters: $p<.05$.

processing (Cabeza et al., 1997). However, focus in the present paper is on structural changes of the medial episodic memory network, which presumably is more vulnerable early in the disease, especially entorhinal cortex and the hippocampus (McDonald et al., 2009). Additional brain areas could be included in the fronto-striatal network, e.g. dorsolateral and lateral orbitofrontal cortices (Alexander et al., 1986). However, morphometric changes with age seem to be strong in the superior frontal cortices, while orbitofrontal and anterior cingulate cortices are relatively spared (Fjell et al., 2009). The superior frontal gyri, especially medial parts, support executive functions (Ridderinkhof et al., 2004).

Lumbar puncture and laboratory analyses

The patients from Study 2 had lumbar puncture (LP) and CSF Total (T)-tau and Aβ42 were examined with a commercially available kit (Innogenetics, Belgium) adapted to a Tecan Robotic Microplate 150 Processor (Tecan AG, Switzerland). Norm values were based on a large sample of healthy controls, and were as follows: Aβ42<550 ng/L, T-tau, >300 ng/L for <50 years, >450 ng/L for 50 to 69 years, and >500 ng/L for >70 years (Sjogren et al., 2001). These cutoff values were decided from a rank-based method, where 0.90 and 0.10 fractiles were estimated to establish reference values for CSF tau and CSF Aβ42, respectively. The CSF analyses were performed at Akershus University Hospital. Parallel analyses with the laboratory at Göteborg University, Sweden, from where the norm values were obtained (Sjogren et al., 2001), were done. Based on these parallel analyses, norm values for Aβ42 were set to 550, to equals 450 from the Göteborg laboratory.

Statistical analyses

Volume and thickness were estimated separately for each hemisphere, and the mean of left and right was used in the analyses to reduce the number of comparisons. Residuals after regression of all volumetric variables on ICV were used as volumetric measures. First, subcortical volumes were compared across AD vs. HE and HE vs. HY by univariate ANOVAs where age was included as covariate. Cortical thickness was compared across groups by fitting a GLM at each vertex with age as covariate. Second, classification accuracy (AD vs. HE, and HE vs. HY), within the two defined neural networks (the medial temporo-parietal vs. the fronto-striatal) was examined by logistic

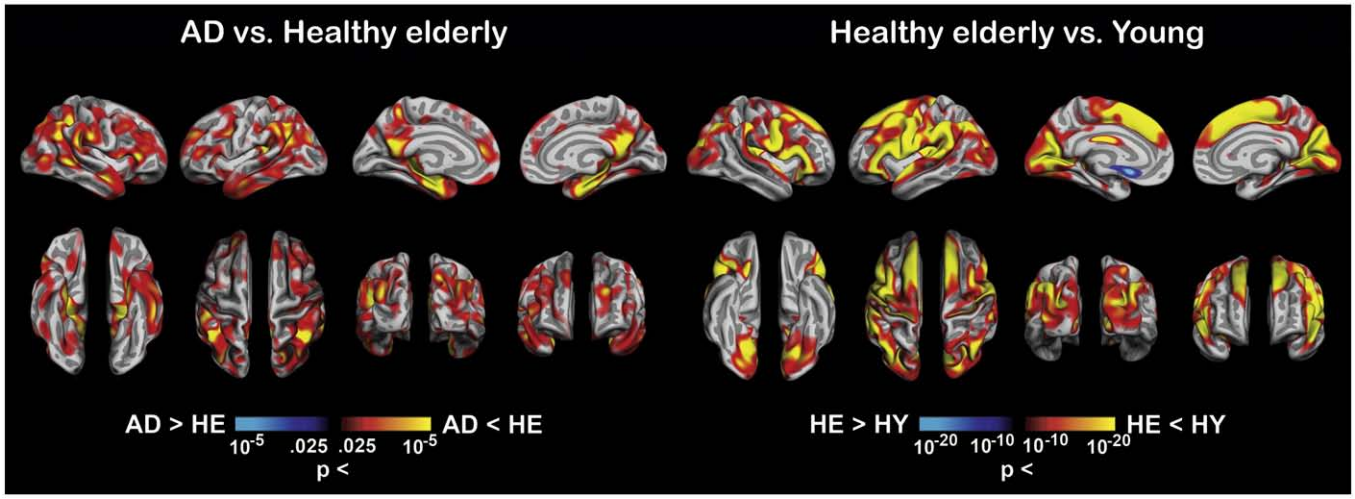

Fig. 2. Effects of AD and healthy aging on cortical thickness. The cortical thickness was compared for AD vs. healthy elderly (HE), and HE vs. healthy young (HY), continuously across the brain surface. The *p*-values are color coded and projected onto the average brain of the sample, which is semi-inflated to better visualize effects in sulci. The *p*-value threshold for the AD vs. HE analysis was set to false discovery rate (FDR)<.05, while the HE vs. young comparisons demanded a more conservative threshold.

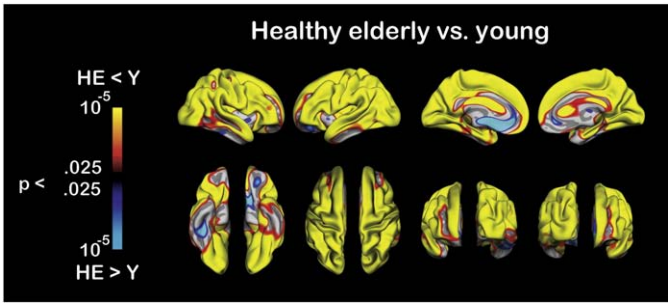

Fig. 3. Effects of healthy aging on cortical thickness. The figure displays the results of the thickness comparison between healthy elderly (HE) and healthy young (HY), by use of the same *p*-value threshold as the one used for the AD vs. HE analysis shown in Fig. 2.

regression analyses where all cortical thickness labels and subcortical volumes within each of the networks were forced into the separate models. Third, exploratory analyses were performed. Forward conditional logistic regression analyses were run with the 16 subcortical (volume) and the 33 cortical (thickness) ROIs entered simultaneously as predictors. This was done to test which constellation of structures best differentiated the groups with an unbiased, hypothesis-free approach. Finally, the regression equations from Study 1 were used to calculate a score for each participant in Study 2 for the medial temporo-parietal and the fronto-striatal networks, as well as for the cluster of structures best distinguishing AD from HE (AD-prone), and HE from HY (aging-prone). Age and scanner site were partialled out, and the scores were correlated with Aβ42 and tau pathology.

Results

Demographics differences between groups

Mean age (76.6 vs. 76.7 for AD vs. HE, $t[187] = -0.93$, $p = .926$) and SES (2.77 vs. 2.50 for AD vs. HE, $t[169] = 1.59$, $p = .11$) did not differ significantly between the AD and HE groups, while a small but statistically significant difference was observed for education (2.81 vs. 3.25 for AD vs. HE, $t[187] = 2.306$, $p = .022$). As SES and education were not available for the young groups, none of these variables were regressed out from the statistical analyses.

Morphometric differences between the groups

ANOVAs were used to compare the subcortical ROIs across the groups, with age used as covariate for the AD vs. HE comparisons (Table 2). All CSF compartments were larger in AD patients than HE, while the volumes of thalamus, putamen, hippocampus, amygdala, accumbens, cerebral WM and cerebral cortex were smaller. CSF compartments were smaller in HY than HE, while all other structures were larger.

The surface-based analysis showed that AD had bilaterally thinner cortex than HE in several areas (Fig. 2) at false discovery rate (FDR) <0.05. The pattern of effects corresponded to known distributions of AD-related cortical thickness differences, and were strongest in the medial temporo-parietal network (entorhinal cortices, posterior cingulate and retrosplenial cortices, parts of precuneus), in addition to inferior and middle temporal and anterior parts of superior temporal cortices as well as the temporal pole, the temporo-parietal junction, and inferior parietal cortex. Smaller and more scattered effects were seen in prefrontal areas. When using the same statistical threshold as in the AD analysis, HE had thinner cortex than HY over the entire cortex except the inferior temporal, anterior parts of cingulate gyrus (where thickening was seen), and the medial orbitofrontal (see Fig. 3). Changing the *p*-value scale to $p<10^{-10}$–10^{-20} revealed topographically differential effects of healthy aging (this scale was chosen to visualize regional heterogeneity of the effects). These were especially strong in prefrontal areas (superior and inferior frontal gyri), superior temporal gyri, the temporo-parietal junction, and posterior areas, including the occipital lobe, cuneus, pericalcarine cortices, and lingual gyri. Only minor effects were seen in the medial temporo-parietal network (entorhinal cortices, posterior cingulate, retrosplenial cortex, and precuneus). The statistical overlays were then binarized (at $p = 10^{-4}$ for AD vs. HE and $p = 10^{-15}$ for HY vs. HE) and projected onto the average brain surface (Fig. 4). There was an almost complete lack of overlap between the effects of AD and the effects of healthy aging. An animation was constructed to show how cortical thickness changes as a function of AD and of normal aging (Supplementary material 1), and snapshots are shown in Fig. 5. Mean thickness in selected ROIs is shown in Fig. 6.

Effects of AD vs. effects of healthy aging: Circuit analyses

A logistic regression model based on all the structures in the medial temporo-parietal network classified AD with a sensitivity of 70.4%, with Nagelkerke's R^2 of .39 ($p < 10^{-12}$). When AD was classified based on the structures in the fronto-striatal network, the sensitivity fell to 60.3% with R^2 of .12. ($p < .001$). When the medial temporo-parietal network was used to distinguish HE from HY, overall classification accuracy was 90.0% with R^2 of .79 ($p < 10^{-40}$).

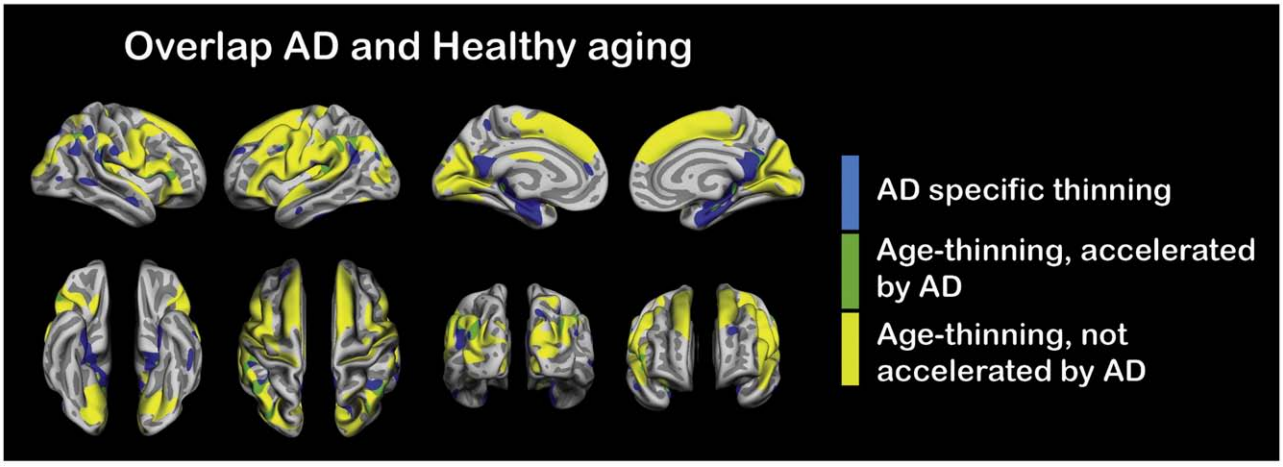

Fig. 4. Overlap between effects of AD and effects of healthy aging. The *p*-value maps from Fig. 3 were binarized at $p = .0001$ for the AD vs. healthy elderly (HE) analysis and $p = 10^{-15}$ for the HE vs. healthy young (HY) analysis, and projected onto the common average brain. Blue indicates AD specific cortical thinning (AD<HE), yellow indicates age-related thinning not accelerated by AD (HE<HY), while green indicates age-related thinning which is accelerated by AD (AD<HE<HY).

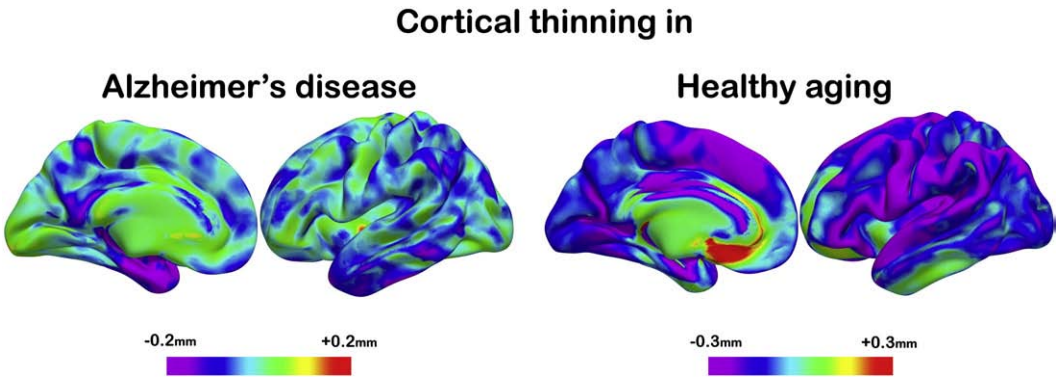

Fig. 5. Differences in cortical thickness between AD, healthy elderly and healthy young. The difference in thickness at each vertex of the cortical surface is color coded, and projected onto the semi-inflated average brain of the total sample. In Supplementary material 1, the changes in thickness associated with the transitions from healthy elderly to AD patients, and the transition from young to elderly controls, are shown as an animation.

Classification accuracy rose to 95.7% with R^2 of .90 ($p < 10^{-53}$) when the fronto-striatal network was used. Thus, while the medial temporo-parietal network best classified AD vs. HE, the fronto-striatal network gave the most accurate classification of HE vs. HY (Supplementary Table 1).

Effects of AD vs. effects of healthy aging: Exploratory cortico-subcortical analyses

All ROIs were included in the same exploratory logistic regression analyses (Fig. 7). For AD vs. HE, six steps yielded an overall correct prediction of 79.9% (76/20 AD and 75/18 HE were correctly/incorrectly classified), with R^2 of .49 (Supplementary Table 2). In this model, the 4th ventricle and hippocampus, and fusiform, retrosplenial, pericalcarine, and supramarginal cortices were included. Pericalcarine and fusiform gyrus had opposite (negative) beta values. This was likely a result of high inter-correlations between the different predictors, yielding opposite weights for some of them in the multivariate analysis. Hippocampus was the first structure to be included, yielding R^2 of .32 and classification accuracy of 70.9%. Adding supramarginal cortices increased accuracy to 75.1% and R^2 to .38. If all structures were forced into the model simultaneously, classification accuracy was 89.9%. It is important to note that due to the inter-correlations between structures within the medial temporo-parietal circuit, few will be chosen as simultaneous predictors in an exploratory analysis. For instance, entorhinal cortex is one of the areas most sensitive to thinning in AD, but due to the high correlation with hippocampal volume ($r = .59$), it was not included in the exploratory model. Thus, degree of overlap between the theory-driven and the exploratory models cannot be used as evidence for or against the validity of the theoretical model.

The same analysis was done for HE vs. HY (Supplementary Table 3). Seven steps yielded an overall correct prediction of 100% ($R^2 = 1$). However, 100% accuracy was reached also after only five steps. In this model, the lateral ventricles and putamen, as well as lateral occipital, lingual, and superior frontal cortices were included. Putamen was the first structure to be included, yielding ^{2} of .74 and overall classification correctness of 90.4%. Adding lingual cortices increased classification accuracy to 94.8% and R^2 to .91.

Validation with CSF biomarker pathology in an independent sample

Of 46 MCI patients, 13 had pathological tau and 9 had pathological Aβ42 values. Tau and Aβ42 pathology did not correlate ($r = .18$, $p = .24$). Betas from the regression equations in Study 1 were used to calculate scores for the medial temporo-parietal and the fronto-striatal circuits for each participant in Study 2. The medial temporo-parietal circuit correlated −.45 ($p < .005$) with tau and −.27 ($p = .075$) with Aβ42 pathology, while the corresponding correla-

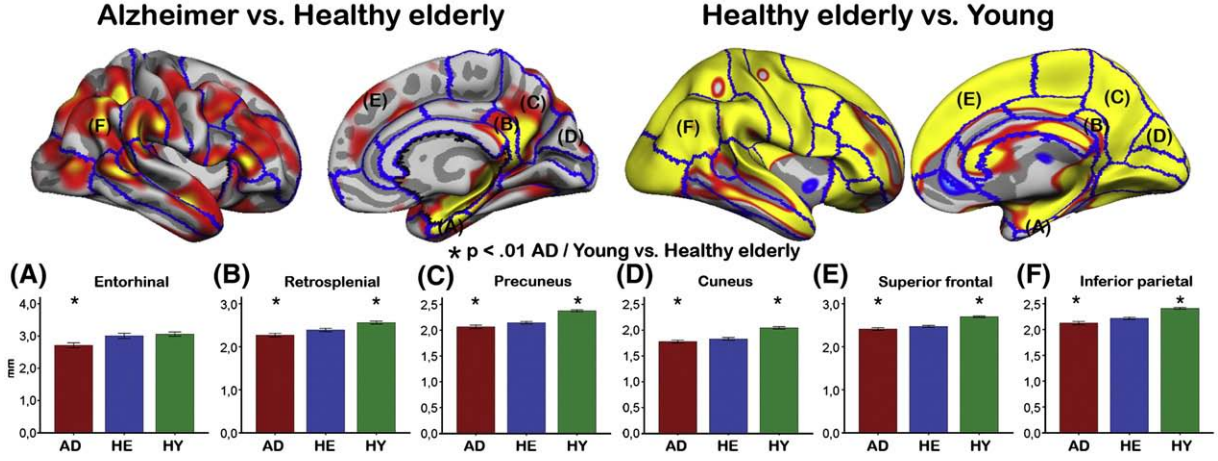

Fig. 6. Mean thickness across groups. The brain surface was parcellated into 33 different gyral-based areas in each hemisphere, and mean thickness in each was calculated. The bars show mean thickness for each group in six areas (error bars represent 95% confidence interval). The mean values of left and right hemisphere are shown. The blue lines indicate the borders between the different cortical areas, shown on the inflated average brain. The statistical maps for AD vs. healthy elderly (HE) are identical to the ones in Fig. 2, while the maps for HE vs. healthy young are the same as the ones in Fig. 3.

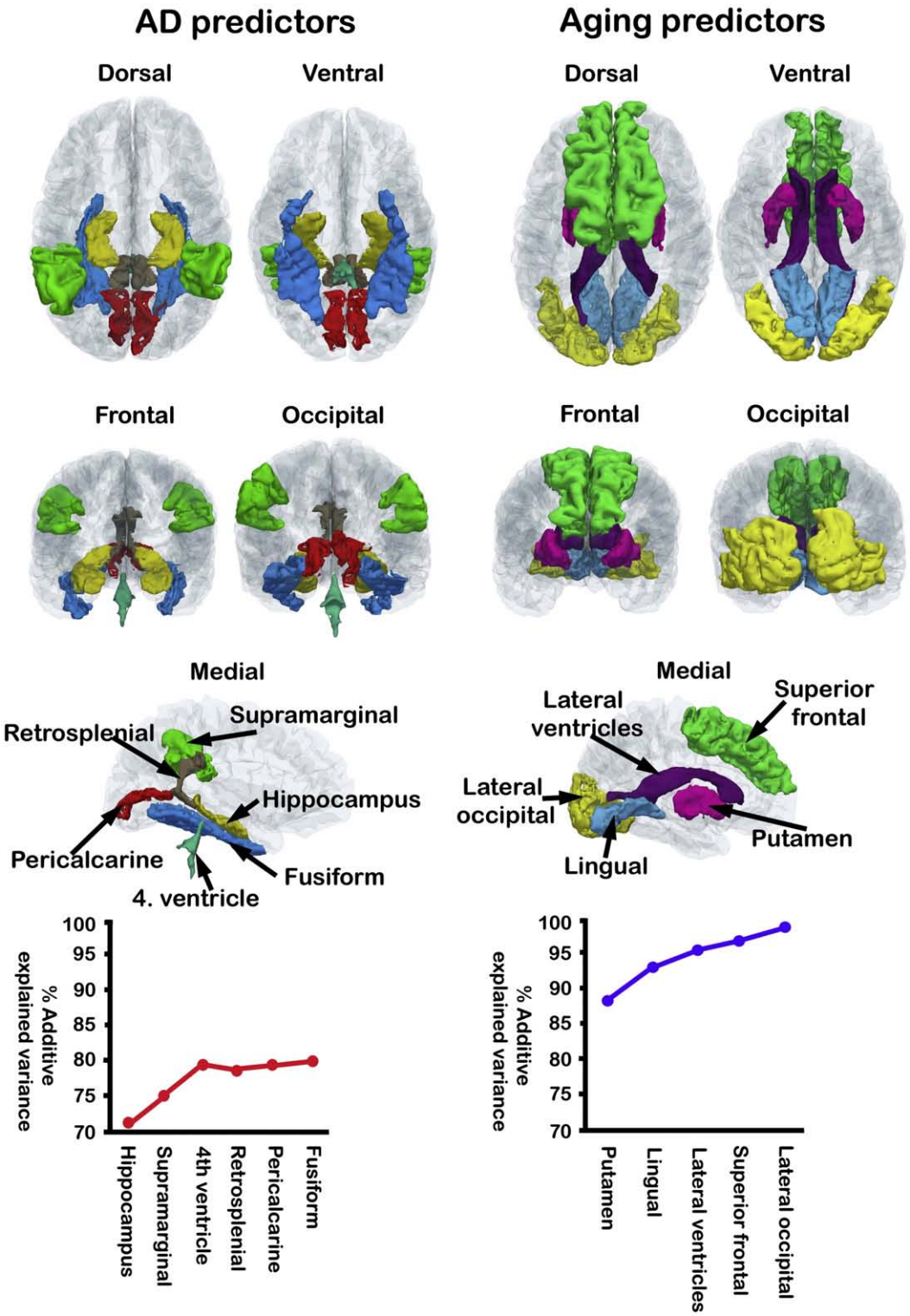

Fig. 7. Results of the cortico-subcortical logistic regression analyses. All cortical regions and subcortical structures were entered into forward conditional logistic regression analyses to test which structures uniquely predicted AD vs. healthy elderly (HE), and HE vs. healthy young (HY). The 3D renderings of the segmentation results for one arbitrary chosen participant are shown to illustrate the structures that were included in the final models, displayed in a transparent brain. As can be seen, there is no overlap between the structures predicting AD vs. HE, and the ones predicting HE vs. HY. The bottom part of the figure shows how the amount of explained variance increased as each of the structures was added to the model.

tions for the fronto-striatal circuit was −.22 ($p = .15$) and −.07 ($p = .64$). The exploratory defined AD-cluster correlated −.40 ($p < .01$) with tau and −.31 ($p < .05$) with Aβ42 pathology, while the aging-cluster did not correlate with any (−.07 and −.09, $p > .57$ for tau and Aβ42, respectively). These results are illustrated in Fig. 8.

Discussion

The present results support the view that the brain areas most vulnerable to the effect of AD are different from those most vulnerable to the process of healthy aging. Compared to healthy

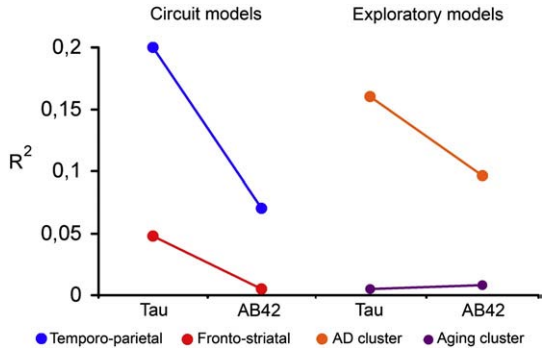

Fig. 8. Correlations with tau and Aβ42 pathology. The figure illustrates the amount of morphometric variance in the two targeted networks, as well as in the two clusters from the explorative analyses, that can be explained by CSF pathology (tau and Aβ42). As can be seen, the medial temporo-parietal network, as well as the AD-prone cluster of structures, was related to CSF biomarker pathology, while the fronto-striatal, as well as the aging-prone cluster, was not.

elderly, the brain structures forming a medial temporo-parietal circuit were substantially smaller or thinner in very mild to moderate AD, while the structures in the fronto-striatal circuit differed less between the groups. Both the medial temporo-parietal and the fronto-striatal network were reduced in healthy elderly compared to young, but the latter to a larger degree. Further, the medial temporo-parietal but not the fronto-striatal circuit was related to pathological levels of tau in an independent sample of MCI patients. Taken together, these findings indicate that brain atrophy in very mild to moderate AD is more than acceleration of non-pathological age processes, and rather represents a unique pattern of degeneration that is not paralleled in healthy aging. The conclusion is coherent with the findings of Head et al. (2004, 2005), who studied hippocampal volume and different parts of the corpus callosum. The present project extended those findings in showing vulnerability of very mild to moderate AD for the medial temporo-parietal network, contrasting these directly with the fronto-striatal network, and showing that the two are differentially related to CSF tau and Aβ42 pathology.

Effects of AD vs. healthy aging on the medial temporo-parietal and fronto-striatal circuits

The present study shows that the pattern of cortico-subcortical effects in very mild to moderate AD and healthy aging deviates from each other in specific ways. The substantial volumetric reductions in the medial temporal part (i.e. hippocampus and entorhinal cortex) of the medial temporo-parietal network in very mild to moderate AD fit with knowledge about the distribution of tau-related pathology. This is initially limited to the entorhinal cortex and adjacent limbic structures, including hippocampus, before spreading to other cortical areas (Braak and Braak, 1991, 1996; Mesulam, 1999). Temporal structures in the medial temporo-parietal network have rich projections to parietal regions (Wagner et al., 2005) and morphometry in this network has been shown to be associated with episodic memory function (Walhovd et al., 2009, 2006, in press; Walhovd et al., 2004; Yonelinas et al., 2007). Specific structures within the network have been shown to undergo degradation in MCI and AD patients (de Leon et al., 1989; Dickerson et al., 2008, 2009; Du et al., 2007; Singh et al., 2006; Whitwell et al., 2007). However, this AD-related atrophy has not previously been directly compared to atrophy in the fronto-striatal network. This network is implicated in executive functions (Buckner, 2004; Head et al., 2004, 2005), and declines substantially even in healthy aging (Fjell et al., 2009; Raz et al., 2003; Westlye et al., 2009). The present results confirm that the medial temporo-parietal network is the one primarily implicated in very mild to moderate AD, while healthy aging is more associated with reductions in the fronto-striatal than the medial temporo-parietal.

The relationship between tau pathology and morphometry in the medial temporo-parietal, but not the fronto-striatal, circuit, validates the results. The circuits were defined in a sample of patients with very mild to moderate AD, and were shown to correlate significantly with tau pathology and almost significantly ($p < .075$) with Aβ42 pathology in a completely independent sample of patients with less severe disease (MCI). Previous studies have shown correlations between hippocampal atrophy and CSF biomarker levels (de Leon et al., 2006; Hampel et al., 2005; Schuff et al., 2009; Sluimer et al., in press), but few studies have looked at the effects outside the temporal lobe. In a sample overlapping with the present, it was shown that correlations between CSF tau and Aβ42 pathology in several regions of interests in medial and lateral temporal and parietal cortex, in addition to hippocampus (Fjell et al., 2008b). A systematic comparison between predefined AD-prone vs. aging-prone networks was not conducted, however.

Even though selective vulnerability for the medial temporo-parietal vs. the fronto-striatal networks was found in very mild to moderate AD vs. healthy aging, it is important to have in mind that age affects the morphometry of almost the entire brain (Fjell et al., 2009; Walhovd et al., in press-b). Thus, brain changes caused by AD are seen on top of changes related to healthy aging. Further, the fronto-striatal network is more reduced in very mild to moderate AD than HE. Still, the medial temporo-parietal network was a better predictor of very mild to moderate AD vs. HE than the fronto-striatal, while the opposite pattern was seen for HE vs. HY. However, it is not likely that a network prone to AD exclusively will ever be identified.

Exploratory analyses: Morphometric changes in specific brain structures in AD and healthy aging

Analyses not restricted to the targeted networks showed that with the exception of the cerebellum, brainstem, caudate and pallidum, all subcortical structures were smaller in very mild to moderate AD than HE. Relationships between AD and amygdala volume fit with neurofibrillary tangles spreading from the hippocampus and entorhinal cortex into basolateral temporal regions, before being manifested in other cortical areas (Braak and Braak, 1996). Thalamic atrophy is probably related to episodic memory deficits in AD patients as part of the Papez circuit (Villain et al., 2008), and the effects on WM volume are in coherence with research demonstrating large effects of MCI and AD on both macro- and micro-structural aspects of WM (Bartzokis et al., 2003; Stoub et al., 2006). Further, the analyses of cortical thickness revealed effects of very mild to moderate AD also outside the medial temporo-parietal network, i.e. in inferior and middle temporal and anterior parts of superior temporal cortices, as well as the temporal pole, the temporo-parietal junction, and inferior parietal cortex, confirming recent findings (Du et al., 2007; Fennema-Notestine et al., 2009; McEvoy et al., 2009; Singh et al., 2006). Dickerson et al. (2008) showed that this pattern of cortical thinning was reliable across multiple samples of MCI/AD patients overlapping with the samples used in the present report (Dickerson et al., 2008), and similar results have been reported from the ADNI study (Alzheimer's Disease Neuroimaging Initiative) (Fennema-Notestine et al., 2009; McEvoy et al., 2009). One study suggested that medial temporal lobe atrophy characterizes MCI, while atrophy in association areas in parietal cortex as well as cingulate cortex, posterior more than anterior, may be a feature of AD (Karas et al., 2004). Thus, although AD seems to be characterized by atrophy in the medial temporo-parietal network, other cortical areas are also vulnerable, especially lateral parietal cortices.

When the subcortical and the cortical ROIs were entered into a stepwise logistic regression analysis, very mild to moderate AD was best classified by a combination of the volume of hippocampus and the 4th ventricle, as well as the thickness of fusiform, retrosplenial, pericalcarine, and supramarginal cortices. Entorhinal cortex and

hippocampus are highly correlated, rendering entorhinal cortex not significant due to shared variance with hippocampus. In contrast, volume change in putamen and the lateral ventricles, together with thinning of superior frontal, lateral occipital and lingual cortices, predicted healthy aging. This highlights that to yield optimal diagnostic accuracy it is necessary to study both cortical and subcortical structures simultaneously, and that very mild to moderate AD and healthy aging are characterized by distinct, non-overlapping patterns of macrostructural brain changes.

The AD-prone cluster of structures was related to CSF biomarker pathology (tau and Aβ42), while the aging-prone cluster was not. This represents additional evidence for a different pattern of morphometric change in AD vs. healthy aging, and suggests that a coherent pattern of effects of AD can be identified across different biomarkers at an early stage of the disease process. Contrary to what was found for the predefined circuits, statistically significant correlations were seen both for tau and Aβ42 pathology. The coefficients were rather similar, however, and not statistically different. It was not surprising that the correlations between CSF biomarkers and brain morphometry were not higher for the theory-driven cluster of five structures compared to the optimal linear combination of structures chosen on the basis of 49 candidates. It is known that levels of CSF tau are increased and levels of CSF Aβ42 are decreased in AD vs. healthy controls (Goedert and Spillantini, 2006; Hampel et al., 2008; Shaw et al., 2009), and the correlations with the AD-prone cluster of structures were not surprising. It is interesting, however, that even though levels of CSF total tau are increased also in healthy aging (Sjogren et al., 2001), no correlations between tau pathology and the aging-prone cluster were seen. In most studies, the CSF-brain morphometry analyses are restricted to gross brain measures (e.g. total brain volume) or parts of the medial temporal lobes, so little prior knowledge exists about the effects of CSF biomarkers on other parts of the brain. The present data indicate that CSF biomarker pathology is related to brain atrophy in areas that are affected in very mild to moderate AD, but not in areas that are as much affected by healthy aging as by AD. The AD pattern of network atrophy grossly replicates the spread of NFT in disease development (Braak and Braak, 1991; Petersen et al., 2006) and correlates with cognitive loss (Fjell et al., 2008a; Giannakopoulos et al., 2003). Degeneration of neural networks may be closely related to mechanisms for disease progression, making the morphometric and molecular mapping of network degeneration in AD even more urgent.

Conclusion

The present study indicates that the pattern of macrostructural brain changes is different in AD vs. healthy aging, and that only the AD-prone areas are correlated with CSF biomarker pathology.

Acknowledgments

This work was funded by the Norwegian Research Council (177404/W50 to K.B.W., 175066/D15 to A.M.F), University of Oslo (to K.B.W. and A.M.F.), and South-Eastern Norway Regional Health Authority (Helse Sør-Øst) and Akershus University Hospital. None of the authors have declared any actual or potential conflicts of interest.

Appendix A. Supplementary data

Supplementary data associated with this article can be found, in the online version, at doi:10.1016/j.neuroimage.2009.09.029.

References

Alexander, G.E., DeLong, M.R., Strick, P.L., 1986. Parallel organization of functionally segregated circuits linking basal ganglia and cortex. Annu. Rev. Neurosci. 9, 357–381.

Allen, J.S., Bruss, J., Brown, C.K., Damasio, H., 2005. Normal neuroanatomical variation due to age: the major lobes and a parcellation of the temporal region. Neurobiol. Aging 26, 1245–1260 discussion 1279-1282.

Arriagada, P.V., Marzloff, K., Hyman, B.T., 1992. Distribution of Alzheimer-type pathologic changes in nondemented elderly individuals matches the pattern in Alzheimer's disease. Neurology 42, 1681–1688.

Auer, S., Reisberg, B., 1997. The GDS/FAST staging system. Int. Psychogeriatr. 9 (Suppl. 1), 167–171.

Bartzokis, G., Cummings, J.L., Sultzer, D., Henderson, V.W., Nuechterlein, K.H., Mintz, J., 2003. White matter structural integrity in healthy aging adults and patients with Alzheimer disease: a magnetic resonance imaging study. Arch. Neurol. 60, 393–398.

Berg, L., 1984. Clinical Dementia Rating. Br. J. Psychiatry 145, 339.

Berg, L., 1988. Clinical Dementia Rating (CDR). Psychopharmacol. Bull. 24, 637–639.

Brayne, C., Calloway, P., 1988. Normal ageing, impaired cognitive function, and senile dementia of the Alzheimer's type: a continuum? Lancet 1, 1265–1267.

Braak, H., Braak, E., 1991. Neuropathological stageing of Alzheimer-related changes. Acta Neuropathol. 82, 239–259.

Braak, H., Braak, E., 1996. Evolution of the neuropathology of Alzheimer's disease. Acta Neurol. Scand. Suppl. 165, 3–12.

Buckner, R.L., 2004. Memory and executive function in aging and AD: multiple factors that cause decline and reserve factors that compensate. Neuron 44, 195–208.

Buckner, R.L., Wheeler, M.E., 2001. The cognitive neuroscience of remembering. Nat. Rev. Neurosci. 2, 624–634.

Buckner, R.L., Head, D., Parker, J., Fotenos, A.F., Marcus, D., Morris, J.C., Snyder, A.Z., 2004. A unified approach for morphometric and functional data analysis in young, old, and demented adults using automated atlas-based head size normalization: reliability and validation against manual measurement of total intracranial volume. NeuroImage 23, 724–738.

Buckner, R.L., Snyder, A.Z., Shannon, B.J., LaRossa, G., Sachs, R., Fotenos, A.F., Sheline, Y.I., Klunk, W.E., Mathis, C.A., Morris, J.C., Mintun, M.A., 2005. Molecular, structural, and functional characterization of Alzheimer's disease: evidence for a relationship between default activity, amyloid, and memory. J. Neurosci. 25, 7709–7717.

Cabeza, R., Kapur, S., Craik, F.I.M., McIntosh, A.R., Houle, S., Tulving, E., 1997. Functional neuroanatomy of recall and recognition: A PET study of episodic memory. J. Cogn. Neurosci. 9, 254–265.

Cousins, D.A., Burton, E.J., Burn, D., Gholkar, A., McKeith, I.G., O'Brien, J.T., 2003. Atrophy of the putamen in dementia with Lewy bodies but not Alzheimer's disease: an MRI study. Neurology 61, 1191–1195.

Dale, A.M., Sereno, M.I., 1993. Improved localization of cortical activity by combining EEG and MEG with MRI cortical surface reconstruction: a linear approach. J. Cogn. Neurosci. 5, 162–176.

Dale, A.M., Fischl, B., Sereno, M.I., 1999. Cortical surface-based analysis. I. Segmentation and surface reconstruction. NeuroImage 9, 179–194.

de Leon, M.J., George, A.E., Stylopoulos, L.A., Smith, G., Miller, D.C., 1989. Early marker for Alzheimer's disease: the atrophic hippocampus. Lancet 2, 672–673.

de Leon, M.J., DeSanti, S., Zinkowski, R., Mehta, P.D., Pratico, D., Segal, S., Rusinek, H., Li, J., Tsui, W., Saint Louis, L.A., Clark, C.M., Tarshish, C., Li, Y., Lair, L., Javier, E., Rich, K., Lesbre, P., Mosconi, L., Reisberg, B., Sadowski, M., DeBernadis, J.F., Kerkman, D.J., Hampel, H., Wahlund, L.O., Davies, P., 2006. Longitudinal CSF and MRI biomarkers improve the diagnosis of mild cognitive impairment. Neurobiol. Aging 27, 394–401.

Desikan, R.S., Segonne, F., Fischl, B., Quinn, B.T., Dickerson, B.C., Blacker, D., Buckner, R.L., Dale, A.M., Maguire, R.P., Hyman, B.T., Albert, M.S., Killiany, R.J., 2006. An automated labeling system for subdividing the human cerebral cortex on MRI scans into gyral based regions of interest. NeuroImage 31, 968–980.

Dickerson, B.C., Bakkour, A., Salat, D.H., Feczko, E., Pacheco, J., Greve, D.N., Grodstein, F., Wright, C.I., Blacker, D., Rosas, H.D., Sperling, R.A., Atri, A., Growdon, J.H., Hyman, B.T., Morris, J.C., Fischl, B., Buckner, R.L., 2008. The cortical signature of Alzheimer's disease: regionally specific cortical thinning relates to symptom severity in very mild to mild AD dementia and is detectable in asymptomatic amyloid-positive individuals. Cereb. Cortex 16, 497–510.

Dickerson, B.C., Feczko, E., Augustinack, J.C., Pacheco, J., Morris, J.C., Fischl, B., Buckner, R.L., 2009. Differential effects of aging and Alzheimer's disease on medial temporal lobe cortical thickness and surface area. Neurobiol. Aging 30 (3), 432–440.

Du, A.T., Schuff, N., Kramer, J.H., Rosen, H.J., Gorno-Tempini, M.L., Rankin, K., Miller, B.L., Weiner, M.W., 2007. Different regional patterns of cortical thinning in Alzheimer's disease and frontotemporal dementia. Brain 130, 1159–1166.

Dubois, B., Feldman, H.H., Jacova, C., Dekosky, S.T., Barberger-Gateau, P., Cummings, J., Delacourte, A., Galasko, D., Gauthier, S., Jicha, G., Meguro, K., O'Brien, J., Pasquier, F., Robert, P., Rossor, M., Salloway, S., Stern, Y., Visser, P.J., Scheltens, P., 2007. Research criteria for the diagnosis of Alzheimer's disease: revising the NINCDS-ADRDA criteria. Lancet Neurol. 6, 734–746.

Edison, P., Archer, H.A., Hinz, R., Hammers, A., Pavese, N., Tai, Y.F., Hotton, G., Cutler, D., Fox, N., Kennedy, A., Rossor, M., Brooks, D.J., 2007. Amyloid, hypometabolism, and cognition in Alzheimer disease: an [11C]PIB and [18F]FDG PET study. Neurology 68, 501–508.

Fennema-Notestine, C., Hagler Jr., D.J., McEvoy, L.K., Fleisher, A.S., Wu, E.H., Karow, D.S., Dale, A.M., 2009. Structural MRI biomarkers for preclinical and mild Alzheimer's disease. Hum. Brain Mapp 30 (10), 3238–3253.

Fischl, B., Dale, A.M., 2000. Measuring the thickness of the human cerebral cortex from magnetic resonance images. Proc. Natl. Acad. Sci. U. S. A. 97, 11050–11055.

Fischl, B., Sereno, M.I., Tootell, R.B., Dale, A.M., 1999. High-resolution intersubject averaging and a coordinate system for the cortical surface. Hum. Brain Mapp. 8, 272–284.

Fischl, B., Salat, D.H., Busa, E., Albert, M., Dieterich, M., Haselgrove, C., van der Kouwe, A., Killiany, R., Kennedy, D., Klaveness, S., Montillo, A., Makris, N., Rosen, B., Dale, A.M., 2002. Whole brain segmentation: automated labeling of neuroanatomical structures in the human brain. Neuron 33, 341–355.

Fischl, B., Salat, D.H., van der Kouwe, A.J., Makris, N., Segonne, F., Quinn, B.T., Dale, A.M., 2004a. Sequence-independent segmentation of magnetic resonance images. NeuroImage 23 (Suppl. 1), S69–84.
Fischl, B., van der Kouwe, A., Destrieux, C., Halgren, E., Segonne, F., Salat, D.H., Busa, E., Seidman, L.J., Goldstein, J., Kennedy, D., Caviness, V., Makris, N., Rosen, B., Dale, A.M., 2004b. Automatically parcellating the human cerebral cortex. Cereb. Cortex 14, 11–22.
Fjell, A.M., Walhovd, K.B., Amlien, I., Bjornerud, A., Reinvang, I., Gjerstad, L., Cappelen, T., Willoch, F., Due-Tonnessen, P., Grambaite, R., Skinningsrud, A., Stenset, V., Fladby, T., 2008a. Morphometric changes in the episodic memory network and tau pathologic features correlate with memory performance in patients with mild cognitive impairment. AJNR Am. J. Neuroradiol. 29, 1183–1189.
Fjell, A.M., Walhovd, K.B., Amlien, I., Bjørnerud, A., Reinvang, I., Gjerstad, L., Cappelen, T., Willoch, F., Due-Tønnessen, P., Grambaite, R., Skinningsrud, A., Stenset, V., Fladby, T., 2008b. Morphometric changes in the episodic memory network and tau pathologic features correlate with memory performance in patients with mild cognitive impairment. Am. J. Neuroradiol. 29, 1–7.
Fjell, A.M., Westlye, L.T., Amlien, I., Espeseth, T., Reinvang, I., Raz, N., Agartz, I., Salat, D.H., Greve, D.N., Fischl, B., Dale, A.M., Walhovd, K.B., 2009. High consistency of regional cortical thinning in aging across multiple samples. Cereb. Cortex 19, 2001–2012.
Folstein, M.F., Folstein, S.E., McHugh, P.R., 1975. "Mini-mental state". A practical method for grading the cognitive state of patients for the clinician. J. Psychiatr. Res. 12, 189–198.
Fotenos, A.F., Snyder, A.Z., Girton, L.E., Morris, J.C., Buckner, R.L., 2005. Normative estimates of cross-sectional and longitudinal brain volume decline in aging and AD. Neurology 64, 1032–1039.
Frisoni, G.B., Lorenzi, M., Caroli, A., Kemppainen, N., Nagren, K., Rinne, J.O., 2009. In vivo mapping of amyloid toxicity in Alzheimer disease. Neurology 72, 1504–1511.
Gauthier, S., Reisberg, B., Zaudig, M., Petersen, R.C., Ritchie, K., Broich, K., Belleville, S., Brodaty, H., Bennett, D., Chertkow, H., Cummings, J.L., de Leon, M., Feldman, H., Ganguli, M., Hampel, H., Scheltens, P., Tierney, M.C., Whitehouse, P., Winblad, B., 2006. Mild cognitive impairment. Lancet 367, 1262–1270.
Giannakopoulos, P., Herrmann, F.R., Bussiere, T., Bouras, C., Kovari, E., Perl, D.P., Morrison, J.H., Gold, G., Hof, P.R., 2003. Tangle and neuron numbers, but not amyloid load, predict cognitive status in Alzheimer's disease. Neurology 60, 1495–1500.
Goedert, M., Spillantini, M.G., 2006. A century of Alzheimer's disease. Science 314, 777–781.
Guillozet, A.L., Weintraub, S., Mash, D.C., Mesulam, M.M., 2003. Neurofibrillary tangles, amyloid, and memory in aging and mild cognitive impairment. Arch. Neurol. 60, 729–736.
Hampel, H., Burger, K., Pruessner, J.C., Zinkowski, R., DeBernardis, J., Kerkman, D., Leinsinger, G., Evans, A.C., Davies, P., Moller, H.J., Teipel, S.J., 2005. Correlation of cerebrospinal fluid levels of tau protein phosphorylated at threonine 231 with rates of hippocampal atrophy in Alzheimer disease. Arch. Neurol. 62, 770–773.
Hampel, H., Burger, K., Teipel, S.J., Bokde, A.L., Zetterberg, H., Blennow, K., 2008. Core candidate neurochemical and imaging biomarkers of Alzheimer's disease. Alzheimers Dement. 4, 38–48.
Han, X., Fischl, B., 2007. Atlas renormalization for improved brain MR image segmentation across scanner platforms. IEEE Trans. Med. Imaging 26, 479–486.
Head, D., Buckner, R.L., Shimony, J.S., Williams, L.E., Akbudak, E., Conturo, T.E., McAvoy, M., Morris, J.C., Snyder, A.Z., 2004. Differential vulnerability of anterior white matter in nondemented aging with minimal acceleration in dementia of the Alzheimer type: evidence from diffusion tensor imaging. Cereb. Cortex 14, 410–423.
Head, D., Snyder, A.Z., Girton, L.E., Morris, J.C., Buckner, R.L., 2005. Frontal–Hippocampal double dissociation between normal aging and Alzheimer's disease. Cereb. Cortex 15, 732–739.
Jack Jr., C.R., Petersen, R.C., O'Brien, P.C., Tangalos, E.G., 1992. MR-based hippocampal volumetry in the diagnosis of Alzheimer's disease. Neurology 42, 183–188.
Karas, G.B., Scheltens, P., Rombouts, S.A., Visser, P.J., van Schijndel, R.A., Fox, N.C., Barkhof, F., 2004. Global and local gray matter loss in mild cognitive impairment and Alzheimer's disease. NeuroImage 23, 708–716.
Kiernan, R.J., Mueller, J., Langston, J.W., Van Dyke, C., 1987. The Neurobehavioral Cognitive Status Examination: a brief but quantitative approach to cognitive assessment. Ann. Intern. Med. 107, 481–485.
Kuperberg, G.R., Broome, M.R., McGuire, P.K., David, A.S., Eddy, M., Ozawa, F., Goff, D., West, W.C., Williams, S.C., van der Kouwe, A.J., Salat, D.H., Dale, A.M., Fischl, B., 2003. Regionally localized thinning of the cerebral cortex in schizophrenia. Arch. Gen. Psychiatry 60, 878–888.
Lerch, J.P., Pruessner, J.C., Zijdenbos, A., Hampel, H., Teipel, S.J., Evans, A.C., 2005. Focal decline of cortical thickness in Alzheimer's disease identified by computational neuroanatomy. Cereb. Cortex 15, 995–1001.
Lerch, J.P., Pruessner, J., Zijdenbos, A.P., Collins, D.L., Teipel, S.J., Hampel, H., Evans, A.C., 2008. Automated cortical thickness measurements from MRI can accurately separate Alzheimer's patients from normal elderly controls. Neurobiol. Aging 29, 23–30.
Marcus, D.S., Wang, T.H., Parker, J., Csernansky, J.G., Morris, J.C., Buckner, R.L., 2007. Open Access Series of Imaging Studies (OASIS): cross-sectional MRI data in young, middle aged, nondemented, and demented older adults. J. Cogn. Neurosci. 19, 1498–1507.
McDonald, C., McEvoy, L.K., Gharapetian, L., Fennema-Notestine, C., Hagler, D.J., Jr., Holland, D., Koyama, A., Dale, A.M., in press. Regional rates of neocortical atrophy from normal aging to early Alzheimer's disease. Neurology.
McEvoy, L.K., Fennema-Notestine, C., Roddey, J.C., Hagler Jr., D.J., Holland, D., Karow, D.S., Pung, C.J., Brewer, J.B., Dale, A.M., 2009. Alzheimer disease: quantitative structural neuroimaging for detection and prediction of clinical and structural changes in mild cognitive impairment. Radiology 251, 195–205.
Mesulam, M.M., 1999. Neuroplasticity failure in Alzheimer's disease: bridging the gap between plaques and tangles. Neuron 24, 521–529.
Morris, J.C., 1993. The Clinical Dementia Rating (CDR): current version and scoring rules. Neurology 43, 2412–2414.
Morris, J.C., Storandt, M., Miller, J.P., McKeel, D.W., Price, J.L., Rubin, E.H., Berg, L., 2001. Mild cognitive impairment represents early-stage Alzheimer disease. Arch. Neurol. 58, 397–405.
Mosconi, L., Brys, M., Glodzik-Sobanska, L., De Santi, S., Rusinek, H., de Leon, M.J., 2007. Early detection of Alzheimer's disease using neuroimaging. Exp. Gerontol. 42, 129–138.
Ohnishi, T., Matsuda, H., Tabira, T., Asada, T., Uno, M., 2001. Changes in brain morphology in Alzheimer disease and normal aging: is Alzheimer disease an exaggerated aging process? AJNR Am. J. Neuroradiol. 22, 1680–1685.
Petersen, R.C., Parisi, J.E., Dickson, D.W., Johnson, K.A., Knopman, D.S., Boeve, B.F., Jicha, G.A., Ivnik, R.J., Smith, G.E., Tangalos, E.G., Braak, H., Kokmen, E., 2006. Neuropathologic features of amnestic mild cognitive impairment. Arch. Neurol. 63, 665–672.
Price, J.L., Morris, J.C., 1999. Tangles and plaques in nondemented aging and "preclinical" Alzheimer's disease. Ann. Neurol. 45, 358–368.
Raz, N., Gunning, F.M., Head, D., Dupuis, J.H., McQuain, J., Briggs, S.D., Loken, W.J., Thornton, A.E., Acker, J.D., 1997. Selective aging of the human cerebral cortex observed in vivo: differential vulnerability of the prefrontal gray matter. Cereb. Cortex 7, 268–282.
Raz, N., Rodrigue, K.M., Kennedy, K.M., Dahle, C., Head, D., Acker, J.D., 2003. Differential age-related changes in the regional metencephalic volumes in humans: a 5-year follow-up. Neurosci. Lett. 349, 163–166.
Raz, N., Rodrigue, K.M., Haacke, E.M., 2007. Brain aging and its modifiers: insights from in vivo neuromorphometry and susceptibility weighted imaging. Ann. NY. Acad. Sci. 1097, 84–93 %R 10.1196/annals.1379.018.
Reisberg, B., Ferris, S.H., de Leon, M.J., Crook, T., 1988. Global Deterioration Scale (GDS). Psychopharmacol. Bull. 24, 661–663.
Ridderinkhof, K.R., Ullsperger, M., Crone, E.A., Nieuwenhuis, S., 2004. The role of the medial frontal cortex in cognitive control. Science 306, 443–447.
Rosas, H.D., Liu, A.K., Hersch, S., Glessner, M., Ferrante, R.J., Salat, D.H., van der Kouwe, A., Jenkins, B.G., Dale, A.M., Fischl, B., 2002. Regional and progressive thinning of the cortical ribbon in Huntington's disease. Neurology 58, 695–701.
Rowe, C.C., Ng, S., Ackermann, U., Gong, S.J., Pike, K., Savage, G., Cowie, T.F., Dickinson, K.L., Maruff, P., Darby, D., Smith, C., Woodward, M., Merory, J., Tochon-Danguy, H., O'Keefe, G., Klunk, W.E., Mathis, C.A., Price, J.C., Masters, C.L., Villemagne, V.L., 2007. Imaging beta-amyloid burden in aging and dementia. Neurology 68, 1718–1725.
Royall, D.R., Mahurin, R.K., Gray, K.F., 1992. Bedside assessment of executive cognitive impairment: the executive interview. J. Am. Geriatr. Soc. 40, 1221–1226.
Salat, D.H., Buckner, R.L., Snyder, A.Z., Greve, D.N., Desikan, R.S., Busa, E., Morris, J.C., Dale, A.M., Fischl, B., 2004. Thinning of the cerebral cortex in aging. Cereb. Cortex 14, 721–730.
Schuff, N., Woerner, N., Boreta, L., Kornfield, T., Shaw, L.M., Trojanowski, J.Q., Thompson, P.M., Jack Jr., C.R., Weiner, M.W., 2009. MRI of hippocampal volume loss in early Alzheimer's disease in relation to ApoE genotype and biomarkers. Brain 132, 1067–1077.
Shaw, L.M., Vanderstichele, H., Knapik-Czajka, M., Clark, C.M., Aisen, P.S., Petersen, R.C., Blennow, K., Soares, H., Simon, A., Lewczuk, P., Dean, R., Siemers, E., Potter, W., Lee, V.M., Trojanowski, J.Q., 2009. Cerebrospinal fluid biomarker signature in Alzheimer's disease neuroimaging initiative subjects. Ann. Neurol. 65, 403–413.
Singh, V., Chertkow, H., Lerch, J.P., Evans, A.C., Dorr, A.E., Kabani, N.J., 2006. Spatial patterns of cortical thinning in mild cognitive impairment and Alzheimer's disease. Brain 129, 2885–2893.
Sjogren, M., Vanderstichele, H., Agren, H., Zachrisson, O., Edsbagge, M., Wikkelso, C., Skoog, I., Wallin, A., Wahlund, L.O., Marcusson, J., Nagga, K., Andreasen, N., Davidsson, P., Vanmechelen, E., Blennow, K., 2001. Tau and Abeta42 in cerebrospinal fluid from healthy adults 21-93 years of age: establishment of reference values. Clin. Chem. 47, 1776–1781.
Sluimer, J.D., Bouwman, F.H., Vrenken, H., Blankenstein, M.A., Barkhof, F., van der Flier, W.M., Scheltens, P., 2008. Whole-brain atrophy rate and CSF biomarker levels in MCI and AD: a longitudinal study. Neurobiol. Aging.
Stoub, T.R., deToledo-Morrell, L., Stebbins, G.T., Leurgans, S., Bennett, D.A., Shah, R.C., 2006. Hippocampal disconnection contributes to memory dysfunction in individuals at risk for Alzheimer's disease. Proc. Natl. Acad. Sci. U. S. A. 103, 10041–10045.
Thal, D.R., Rub, U., Orantes, M., Braak, H., 2002. Phases of A beta-deposition in the human brain and its relevance for the development of AD. Neurology 58, 1791–1800.
Thompson, P.M., Hayashi, K.M., de Zubicaray, G., Janke, A.L., Rose, S.E., Semple, J., Herman, D., Hong, M.S., Dittmer, S.S., Doddrell, D.M., Toga, A.W., 2003. Dynamics of gray matter loss in Alzheimer's disease. J. Neurosci. 23, 994–1005.
Thompson, P.M., Hayashi, K.M., Dutton, R.A., Chiang, M.C., Leow, A.D., Sowell, E.R., De Zubicaray, G., Becker, J.T., Lopez, O.L., Aizenstein, H.J., Toga, A.W., 2007. Tracking Alzheimer's disease. Ann. N. Y. Acad. Sci. 1097, 183–214.
Villain, N., Desgranges, B., Viader, F., de la Sayette, V., Mezenge, F., Landeau, B., Baron, J.C., Eustache, F., Chetelat, G., 2008. Relationships between hippocampal atrophy, white matter disruption, and gray matter hypometabolism in Alzheimer's disease. J. Neurosci. 28, 6174–6181.
Wagner, A.D., Shannon, B.J., Kahn, I., Buckner, R.L., 2005. Parietal lobe contributions to episodic memory retrieval. Trends Cogn. Sci. 9, 445–453.

Walhovd, K.B., Fjell, A.M., Reinvang, I., Lundervold, A., Fischl, B., Quinn, B.T., Dale, A.M., 2004. Size does matter in the long run: hippocampal and cortical volume predict recall across weeks. Neurology 63, 1193–1197.

Walhovd, K.B., Fjell, A.M., Dale, A.M., Fischl, B., Quinn, B.T., Makris, N., Salat, D., Reinvang, I., 2006. Regional cortical thickness matters in recall after months more than minutes. NeuroImage 31, 1343–1351.

Walhovd, K.B., Fjell, A.M., Amlien, I., Grambaite, R., Stenset, V., Bjornerud, A., Reinvang, I., Gjerstad, L., Cappelen, T., Due-Tonnessen, P., Fladby, T., 2009. Multimodal imaging in mild cognitive impairment: metabolism, morphometry and diffusion of the temporal-parietal memory network. NeuroImage 45, 215–223.

Walhovd, K.B., Fjell, A.M., Dale, A.M., McEvoy, L.K., Brewer, J., Karow, D.S., Salmon, D.P., Fennema-Notestine, C., 2009a. Multi-modal imaging predicts memory performance in normal aging and cognitive decline. Neurobiol. Aging.

Walhovd, K.B., Westlye, L.T., Amlien, I., Espeseth, T., Reinvang, I., Raz, N., Agartz, I., Salat, D.H., Greve, D.N., Fischl, B., Dale, A.M., Fjell, A.M., 2009b. Consistent neuroanatomical age-related volume differences across multiple samples. Neurobiol. Aging.

Wallin, A., Edman, A., Blennow, K., Gottfries, C.G., Karlsson, I., Regland, B., Sjogren, M., 1996. Stepwise comparative status analysis (STEP): a tool for identification of regional brain syndromes in dementia. J. Geriatr. Psychiatry Neurol. 9, 185–199.

Westlye, L.T., Walhovd, K.B., Dale, A.M., Espeseth, T., Reinvang, I., Raz, N., Agartz, I., Greve, D.N., Fischl, B., Fjell, A.M., 2009. Increased sensitivity to effects of normal aging and Alzheimer's disease on cortical thickness by adjustment for local variability in gray/white contrast: A multi-sample MRI study. NeuroImage.

Whalley, L.J., 2002. Brain ageing and dementia: what makes the difference? Br. J. Psychiatry 181, 369–371.

Whitwell, J.L., Przybelski, S.A., Weigand, S.D., Knopman, D.S., Boeve, B.F., Petersen, R.C., Jack Jr., C.R., 2007. 3D maps from multiple MRI illustrate changing atrophy patterns as subjects progress from mild cognitive impairment to Alzheimer's disease. Brain 130, 1777–1786.

Yonelinas, A.P., Widaman, K., Mungas, D., Reed, B., Weiner, M.W., Chui, H.C., 2007. Memory in the aging brain: doubly dissociating the contribution of the hippocampus and entorhinal cortex. Hippocampus 17, 1134–1140.